Physiologia Plantarum
An International Journal for Plant Biology

Sterol partitioning by *HMGR* and *DXR* for routing intermediates toward withanolide biosynthesis

Shefali Singh[a,†], Shaifali Pal[a,†], Karuna Shanker[b], Chandan Singh Chanotiya[b], Madan Mohan Gupta[b], Upendra Nath Dwivedi[c] and Ajit Kumar Shasany[a,*]

[a]Biotechnology Division, CSIR – Central Institute of Medicinal and Aromatic Plants, Lucknow 226015, UP, India
[b]Analytical Chemistry Division, CSIR – Central Institute of Medicinal and Aromatic Plants, Lucknow 226015, UP, India
[c]Department of Biochemistry, University of Lucknow, Lucknow, 226007, UP, India

Correspondence
*Corresponding author,
e-mail: ak.shasany@cimap.res.in,
akshasany@yahoo.com

Received 31 January 2014;
revised 11 March 2014

doi:10.1111/ppl.12213

Withanolides biosynthesis in the plant *Withania somnifera* (L.) Dunal is hypothesized to be diverged from sterol pathway at the level of 24-methylene cholesterol. The conversion and translocation of intermediates for sterols and withanolides are yet to be characterized in this plant. To understand the influence of mevalonate (MVA) and 2-C-methyl-D-erythritol-4-phosphate (MEP) pathways on sterols and withanolides biosynthesis in planta, we overexpressed the *WsHMGR2* and *WsDXR2* in tobacco, analyzed the effect of transient suppression through RNAi, inhibited MVA and MEP pathways and fed the leaf tissue with different sterols. Overexpression of *WsHMGR2* increased cycloartenol, sitosterol, stigmasterol and campesterol compared to *WsDXR2* transgene lines. Increase in cholesterol was, however, marginally higher in *WsDXR2* transgenic lines. This was further validated through transient suppression analysis, and pathway inhibition where cholesterol reduction was found higher due to *WsDXR2* suppression and all other sterols were affected predominantly by *WsHMGR2* suppression in leaf. The transcript abundance and enzyme analysis data also correlate with sterol accumulation. Cholesterol feeding did not increase the withanolide content compared to cycloartenol, sitosterol, stigmasterol and campesterol. Hence, a preferential translocation of carbon from MVA and MEP pathways was found differentiating the sterols types. Overall results suggested that MVA pathway was predominant in contributing intermediates for withanolides synthesis mainly through the campesterol/stigmasterol route in planta.

Introduction

Withania somnifera (L.) Dunal is an important perennial medicinal plant of family Solanaceae. Different parts of this plant (root, leaf, berries, bark) are used traditionally as potent drug in various indigenous systems of medicine for over 3000 years. Its pharmacological and therapeutic efficacy has also been established for antioxidant, anxiolytic, adaptogenic, memory enhancing, antiparkinsonian, antivenom, antiinflammatory, immune-modulating, antistress and antitumor properties (Ray and Gupta 1994, Dhuley

Abbreviations – MEP, 2-C-methyl-D-erythritol-4-phosphate; MVA, mevalonate; N-J, Neighbor-Joining; RNAi, RNA interference; RQ, relative quantity; *WsDXR*, *Withania somnifera* 1-deoxy-D-xylulose 5-phosphate reductoisomerase; *WsHMGR*, *Withania somnifera* 3-hydroxy-3-methylglutaryl coenzyme A reductase.

†These authors contributed equally to this work.

2001, Winters 2006, Gupta and Rana 2007, Mirjalili et al. 2009). Withanolides biosynthesized by the plant are C_{28}-steroidal lactones of triterpene ancestry (Misra et al. 2008), wherein C-22 and C-26 are appropriately oxidized to form a δ-lactone ring called 22-hydroxy ergostane-26-oic acid 26, 22-δ-lactone. The biosynthetic route is hypothesized to be diverged from sterol pathway at the level of 24-methylene cholesterol (Sangwan et al. 2008). Though subsequent conversion of 24-methylene cholesterol into withaferin A and other withanolides is yet to be biochemically characterized, it is predicted to be a multistep process involving hydroxylation, oxidation, cyclization steps (Lockley et al. 1976, Velde and Lavie 1982, Sangwan et al. 2008). Recently, biochemical and molecular studies have been initiated to elucidate the pathways for various withanolides in *W. somnifera* (Sharma et al. 2007, Madina et al. 2007, Senthil et al. 2010, Gupta et al. 2011, 2013a, Pal et al. 2011). Gupta et al (2013b) have reported de novo assembly of *W. somnifera* leaf and root transcriptomes to identify putative genes involved in the withanolides biosynthesis. Also, an efficient genetic transformation system has been developed for the plant (Pandey et al. 2010) and full-length FPPS cDNA was characterized (Gupta et al. 2011). Chaurasiya et al. (2012) analyzed the contribution of isoprenes from mevalonate (MVA) and 2-C-methyl-D-erythritol-4-phosphate (MEP) pathway for Withaferin A biogenesis through a NMR-based study by tracing of ^{13}C label from $^{13}C1$-D-glucose to withaferin A in microshoot cultures of the plant and concluded a relative contribution of 75:25. But, this report does not describe the carbon contribution for other withanolides.

Sterol biosynthesis in plants results in the production of sitosterol, stigmasterol and campesterol as major products (Fig. 1). Several studies with radiolabeled precursors have demonstrated that cycloartenol, 24-methylene cycloartenol, cycloeucalenol and obtusifoliol are primary intermediates in the biosynthesis of phytosterols (Kahn et al. 1996). All isoprenoids, including the phytosterols, are known to be biosynthesized from two common C5 isoprene units: isopentenyl diphosphate (IPP) and its isomer, dimethylallyl diphosphate (DMAPP) via cytosolic MVA and plastidial MEP pathways (Lichtenthaler 1999; Rohmer 1999; Suzuki and Muranaka 2007). Also, DXR and HMGR are described to be the key enzymes that regulate the carbon flux through MEP and MVA pathway respectively (Botella-Pavia et al. 2004, Dubey et al. 2003, Carretero-Paulet et al. 2006).

Hence, it is essential to investigate the translocation of intermediates toward withanolides in planta as these two primary pathways channelize carbon to a diverse array of molecules under the influence of several internal and external factors. Expression of *WsDXR* (*WsDXR1*) is reported to be higher in leaf tissues compared to the root (Gupta et al. 2013a) whereas *WsHMGR* (*WsHMGR1*) expression is maximum in the flower followed by root tissue (Akhtar et al. 2012). Since withanolides are found in both leaf and root but the major source is the leaf (Glotter 1991, Jayaprakasam and Nair 2003, Mirjalili et al. 2009), in the present investigation we functionally characterized 1-deoxy-D-xylulose-5-phosphate reductoisomerase (*WsDXR2*) and hydroxymethylglutaryl-CoA reductase (*WsHMGR2*) genes from *W. somnifera* leaf (Pal et al. 2011) with high expression in the leaf with the objective to follow the metabolite translocation in planta. These genes were individually overexpressed in a heterologous system to analyze the relative contribution of carbon from these two pathways toward sterols. RNAi (RNA interference) constructs of these two genes were transiently expressed in *W. somnifera* leaf to correlate the carbon partitioning during withanolides synthesis. In addition, fosmidomycin and mevinolin inhibition of MEP and MVA pathways respectively indicated the relative contribution of intermediates (Fig. 1). Finally, sterol feeding assay confirmed the involvement of sterols for withanolide biosynthesis. The results of this study have explicitly demonstrated for the first time the relative contribution of MVA and MEP pathways in carbon channeling toward withanolides biosynthesis via sterol metabolism in *W. somnifera*.

Materials and methods

Plant material

Withania somnifera var. CIM Poshita seeds and plants were obtained from National Gene Bank for Medicinal and Aromatic Plants (NGBMAP) maintained at CSIR – Central Institute of Medicinal and Aromatic Plants in Lucknow, India. Seeds were sown in mid-July for raising nursery. After sowing, a mixture of farm yard manure (FYM) and soil was thinly spread over the seeds and irrigated with a sprinkler hose. The seeds took 8–10 days to germinate and seedlings were ready for transplantation in 5 weeks. Transplantation of seedlings was carried out in plots of 10.0×10.0 m size with 10×20 cm row to row and plant to plant spacing. A light irrigation just after the planting ensured establishment of seedlings. The established plants were also maintained under glasshouse conditions, i.e. 60–75% relative humidity and 25 ± 2°C temperature. *Nicotiana tabacum* L. var Xanthi was used in transformation experiments.

Phylogenetic analysis

Amino acid sequences of *HMGR* and *DXR* from different species were aligned and phylogeny was reconstructed

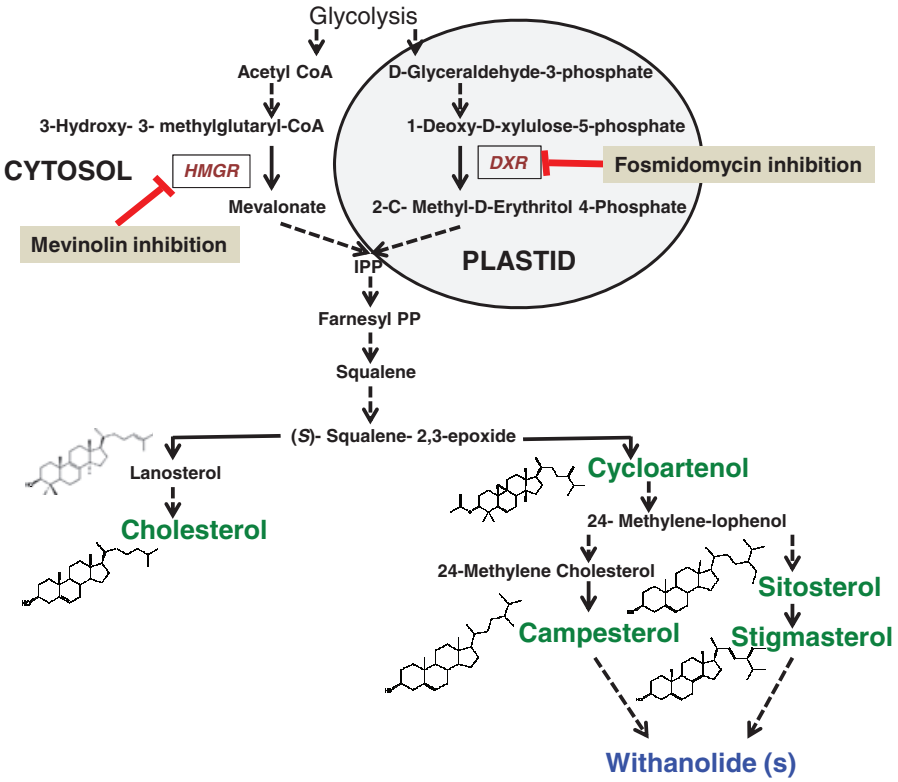

Fig. 1. Withanolide biosynthesis pathway through sterol. The withanolide biosynthesis is extrapolated from the inferences of all the results. Shows sites of action for mevinolin and fosmidomycin inhibition.

using Bootstrap Neighbor-Joining (N-J) distance method of CLUSTAL X version 2.0.11 (Thompson et al. 1997). TREEVIEW software, version 1.6.6 was used to view the resulting bootstrap N-J tree (Saitou and Nei 1987).

Sterol extraction and analysis

A modified method of Darnet and Rahier (2004) was used to prepare plant extract for sterol analysis. Freeze-dried leaves (200 mg) were ground to fine powder and homogenized in 5 ml of methanol/KOH (6%, w/v) and heated at 80°C under reflux for 2 h. The mixture was diluted with one volume of water and total sterol was extracted three times with three volumes of n-hexane. The extract was dried on Na_2SO_4, evaporated to dryness and subjected to GC analysis according to Liu et al (2007) after dissolving in 500 µl dichloromethane from which 1 µl was injected for analysis. Gas chromatography was performed in Agilent Technologies series 7890A equipment (Agilent Technologies, Wilmington, DE) having G4513A automated sampler injection system, split/splitless injector, 30 m (length) × 0.320 mm (diameter) × 0.25 µm film thickness HP-5 fuse-silica capillary column coated with 5% phenylmethyl siloxane and a flame ionization detection (FID) controlled by the AGILENT EZ CHROME-ELITE 3.3.2SP2 software. The oven temperature was adjusted to 240°C for 10 min and raised to 260°C with an increment of 2°C min^{-1} and maintained at 260°C for 30 min with the injection port at 270°C and detector at 300°C. The split ratio was 15:1 with nitrogen as the carrier gas at a flow rate of 1.0 ml min^{-1}. Estrone was used as internal standard. All other reference molecules like cholesterol, campesterol, stigmasterol, β-sitosterol and cycloartenol were purchased from SIGMA. GC-MS analysis was carried out in PerkinElmer AutoSystem XL GC (PerkinElmer, Waltham, MA), interfaced with a Turbomass Quadrupole mass spectrometer using VF-1 ms (15 m × 0.25 mm i.d., 0.25 µm film thickness) FSCAP with H_2 as carrier gas at 8 psi constant pressure. The column oven was programmed from 150 to 300°C at the rate of 5°C min^{-1}. Injector temperature was 280°C, transfer line and source temperatures were 250°C; ionization energy 70 eV; scan time 1 s; inter scan delay 0.1; mass scan range 40–500 amu with a split ratio of 50. Compounds were identified by co-injection of standards and searching mass spectral database.

Withanolide extraction and analysis

Withanolide content was estimated by HPLC (Scartezzini 2007, Srivastava et al. 2008). For this, dried plant material (200 mg) was powdered, extracted with 10 ml warm (50°C) methanol for 4 h, and filtered through a Whatman No. 1 filter paper. This process was repeated three times and the combined methanol extract was concentrated under vacuum for HPLC analysis. A Spherisorbs® C18 (250 mm × 4.6 mm i.d.) 10 μm particle size ODS2 column (Waters, Milford, MA) was used with a 40:60 (v/v) mix of acetonitrile: 0.1% (v/v) trifluoroacetic acid in water as the mobile phase. The flow rate was 1.0 ml min^{-1}, and the detector wavelength was 220 nm. All standard withanolides were purchased from ChromaDex (Irvine, CA).

Semi-quantitative and quantitative RT-PCR

Semi-quantitative RT-PCR (ThermoScript™ RT-PCR kit; Invitrogen, Carlsbad, CA) was carried out using total RNA, gene specific primers and compared with *β*-actin amplification. The expression levels of *WsDXR2* and *WsHMGR2* under various conditions were also measured by real-time PCR with SYBR green I chemistry (Applied Biosystems, Carlsbad, CA) following the protocol described by Misra et al. (2012). The primer sequences are provided in Appendix S1. Threshold cycle (Ct) values obtained after real-time PCR were used for calculation of ΔCt (target-endogenous control). The quantification was carried out by calculation of ΔΔCt to determine the fold difference in gene expression [Δ Ct target − Δ Ct calibrator]. Relative quantity (RQ) was determined by $2^{-\Delta\Delta Ct}$.

WsDXR2 and *WsHMGR2* genes

Both, 1-deoxy-D-xylulose-5-phosphate reductoisomerase (*WsDXR2*, GQ921844) and the hydroxy methylglutaryl-CoA reductase (*WsHMGR2*, GQ921845) genes were isolated by RT-PCR approach using the ThermoScript RT-PCR system (Invitrogen) and degenerate primers as reported earlier (Pal et al. 2011). Cluster analysis of these genes was carried out according to Misra et al (2012).

Preparation of overexpression gene constructs and transgenic tobacco plants

*Xba*I (forward primer) and *Bam*HI (reverse primer) restriction sites were introduced at either sides of the *WsDXR2* coding sequence where as *Bam*HI (forward primer) and *Hind* III (reverse primer) restriction sites were introduced on either side of the truncated *WsHMGR2* containing coding sequence (without the first 252 nucleotides, i.e. 84 amino acids). These amplified PCR-products were cloned in pGEM®-T Easy vector (Promega, Madison, WI) and sequence confirmed. The plasmid containing the *WsDXR2* coding region was digested with *Xba*I and *Sac*I (*Sac*I site present in pGEM-T Easy vector) and introduced between the 35S promoter and *nos* terminator of restricted pBI121 replacing *GUS* gene to yield the final construct PBI-*WsDXR2*. Because of the *Sac*I restriction site inside *WsHMGR2* (1476) a different approach was followed for *WsHMGR2* overexpression construct. The plasmid containing the truncated *WsHMGR2* coding region and PBI121 vector were restricted with *Hin*dIII and *Sac*I restriction enzyme respectively and blunted using T4 DNA polymerase (New England Biolab, Ipswich, MA). Both the linearized plasmids (pGEM-T Easy vector containing *WsHMGR2* and pBI121) were restricted with *Bam*HI. This released the *WsHMGR2* fragment and pBI121 (having *Bam*HI at one end and blunted at the other) which were eluted and ligated to obtain pBI-*WsHMGR2* between the CaMV 35S promoter and nopaline synthase (*nos*) poly(A) signal. The binary vectors with and without the transgene (*WsDXR2* and *WsHMGR2*) were transformed into GV3103 strain of *Agrobacterium* separately. The transformation method as described earlier (Horsch et al. 1985, Luo et al. 2006) was used to generate transgenic tobacco plant overexpressing these genes. Regenerants were observed after 3–4 weeks of selection on kanamycin (200 μg ml^{-1}). Regenerated shoots were excised and rooted. Plantlets with well-established root system were hardened for 2 weeks, subsequently transferred to soilrite mix and irrigated with diluted MS liquid medium. Fully acclimatized plantlets were grown in the greenhouse. For transcript and sterol analysis, three transgenic lines for each gene were randomly selected after 9 weeks.

Preparation of RNAi constructs and transient suppression

RNAi constructs of the *WsHMGR2* and *WsDXR2* fragments were prepared through pHANNIBAL cloning vector (CSIRO, Australia). Both the sense and antisense fragments of 496 bp (corresponding to positions 1–496) from *WsDXR2* coding region and 479 bp (corresponding to positions 1–479) from *WsHMGR2* coding region were cloned in pHANNIBAL. For the sense constructs, the primers designed were having *Xho*I/*Eco*RI (*WsDXR2*) and *Xho*I/*Kpn*I (*WsHMGR2*) restriction sites and for the antisense constructs, the primers used were having *Bam*HI/*Xba*I (*WsDXR2*, *WsHMGR2*) restriction sites (Appendix S1). Restriction sites added by the primers ensured the correct orientation of the resulting sense

and antisense constructs to get the two arms of the hairpin. The hairpin cassette was cloned in pART27 binary vector in a single step using the *Not*I restriction site. The binary vectors with and without the hairpin cassette were then transformed into GV3103 strain of *Agrobacterium* separately. Binary vectors containing RNAi construct for *WsHMGR2* was named as pART27: *WsHMGR2i* and RNAi construct containing *WsDXR2* as pART27:*WsDXR2i*. Infiltration was carried out as per the protocol of Ratogi et al. (2013). Before starting the leaf infiltration, the 12-week-old plantlets were sprayed with water to let the stomata open. Three to four leaved stem twigs or leaves were infiltrated with *Agrobacterium* containing the RNAi constructs. After confirming the infiltration by visual inspection (infiltrated areas of the leaf become translucent when observed against a source of light, these patches were marked), the plant twigs were kept in 4% sucrose, covered by pricked cling film for aeration, incubated in dark at 24°C for 72 h. Total RNA was isolated from marked patches of the leaves and samples were dried to analyze the withanolides. Sterol analysis was carried out from the complete leaf without dissecting the patches.

Assay of HMGR and DXR enzymes in transgenic tobacco plant

Intact chloroplasts were isolated from young leaves of 9-week-old tobacco plants using the Chloroplast Isolation Kit (Sigma). These were suspended in 500 µl of assay buffer containing 150 m*M* Tris–HCl (pH 7.2), 5 m*M* $MgCl_2$, 5 m*M* β-mercaptoethanol and 1 m*M* thiamine diphosphate. After centrifugation (15 000 *g*, 30 min), the supernatant (stroma fraction) was used to assay DXR activity. DXP (1-deoxy-D-xylulose 5-phosphate) is the known substrate of DXR which is converted to MEP (2-C-methylerythritol 4-phosphate) by an NADPH dependent reduction (Takahashi et al. 1998). Hence, DXR activity was determined in 1 ml of assay buffer containing chloroplast stroma protein (0.1 mg), 1 m*M* DXP (Sigma) and 1 m*M* $MnCl_2$. The reaction was initiated by adding NADPH to a final concentration of 0.125 m*M* and oxidation of NADPH was monitored with a spectrophotometer at 340 nm for 10 min at 25°C, assuming an absorption coefficient of 6.22 mM^{-1} cm^{-1} (Miller et al. 2000, Hasunuma et al. 2008). Control reaction was performed in the absence of cell-free extracts. HMGR was extracted from the fresh leaves in an extraction buffer containing 50 m*M* Tris–HCl, 10 m*M* β-mercaptoethanol, 1% (w/v) polyvinylpyrrolidone (PVP) at pH 7.5. HMGR was extracted following Mansouri et al. (2009) and the activity was determined by the method of Toroser and Huber (1998). Briefly, the enzyme extract (0.5 mg) was added to 1 ml 50 m*M* Tris–HCl assay buffer (pH 7.0) containing 0.3 m*M* HMG-CoA (Sigma), 0.2 m*M* NADPH and 4 m*M* dithiothreitol. NADPH oxidation in the reaction solution was monitored at 25°C by the decreasing absorbance at 340 nm, against the solution free of HMG-CoA as a blank. One HMGR enzyme unit was calculated as equivalent to the oxidation of 1 m*M* of NADPH per minute (Ge and Wu 2005, Mansouri et al. 2009). The extinction coefficient for NADPH at 340 nm is 6.22 mM^{-1} cm^{-1}. Protein concentration was analyzed following the method described by Bradford (1976) with bovine serum albumin (BSA) as a standard.

Inhibitor assay for DXR and HMGR

Small twigs containing four to five leaves (from 5 to 6 week old plants) were used in this study. Twigs were collected and dipped in 0.5 µg ml^{-1} solution of fosmidomycin (in water) and mevinolin (in DMSO) separately. Twigs dipped in MilliQ water/DMSO were used as a control. After 24 h of incubation samples were collected and used for HPLC analysis to detect withanolides and GC for sterol analysis. For HPLC and GC analysis 100 mg (dry weight) sample was used. The percent increase in withanolide content was calculated comparing the respective controls from three biological replicates.

Sterol feeding assay

Leaves from 5 to 6 week old single plant of *W. somnifera* were used in this experiment. For each treatment 1.5 g leaf sample was cut into pieces to approximately 0.2–0.4 mm size. Cut leaf samples were dipped in cholesterol, stigmasterol, sitosterol, campesterol, cycloartenol (0.5 mg/10 ml sterile MilliQ water) and kept for 2 h at room temperature with constant shaking (50 rpm). Cut leaf samples dipped in MilliQ water were used as a control. Subsequently, samples were collected, washed thoroughly with MilliQ water, dried for 2 days at 42°C, ground to fine powder and 100 mg was used for HPLC analysis to quantify withanolides. The analysis was carried out with three biological replicates.

Results

WsHMGR2 and *WsDXR2*

In the amino acid sequence alignment (Fig. 2), *WsHMGR2* (GQ921845) clustered with *Capsicum annuum* HMGR2 (Q9XEL8.1) whereas *WsHMGR1* (HQ293119) clustered separately. This isoform expressed more in the matured leaf compared to the younger leaf and

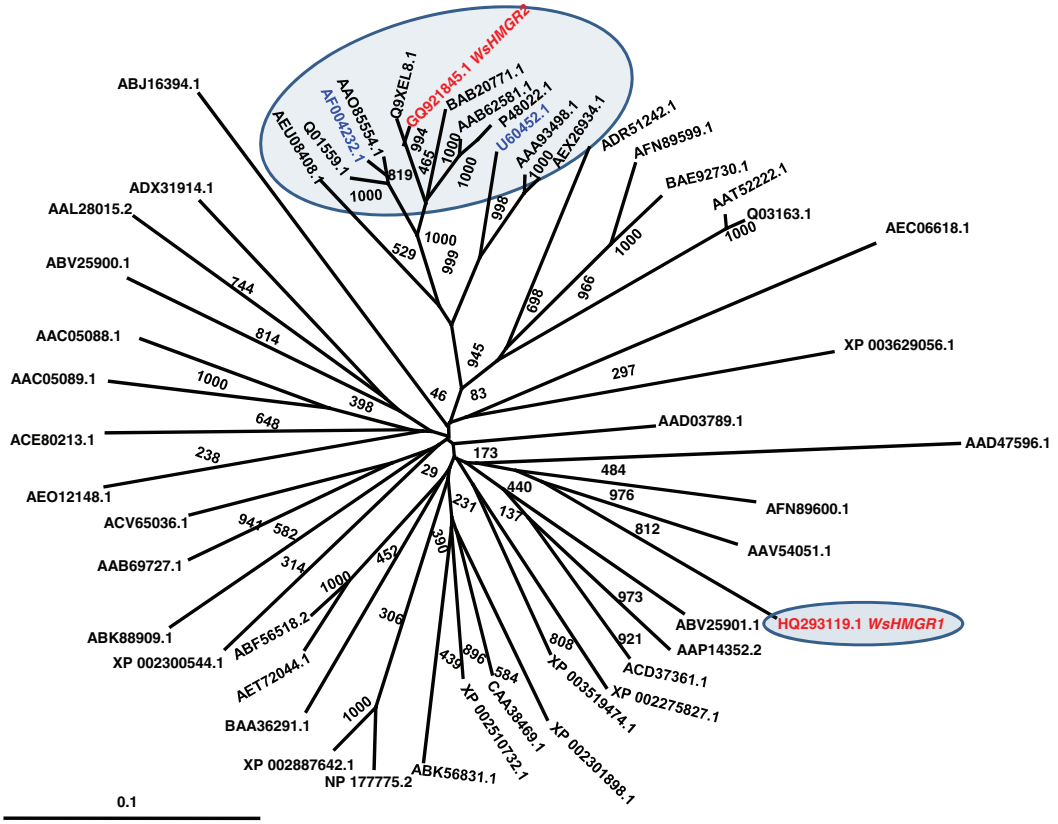

Fig. 2. Unrooted N-J tree comparing the amino acid sequences of *Withania somnifera* (*WsHMGR2*) with *HMGR*s reported from other species. GenBank accession numbers for the corresponding amino acid sequences are: *Andrographis paniculata* (AAL28015.2), *Andrographis paniculata* (AAP14352.2), *Antirrhinum majus* (ABV25901.1), *Arabidopsis lyrata* (XP_002887642.1), *Arabidopsis thaliana* (AEC06618.1), *Arabidopsis thaliana* (NP_177775.2), *Artemisia annua* (AAD47596.1), *Atractylodes lancea* (ABK88909.1), *Bacopa monnieri* (ADX31914.1), *Camellia sinensis* (AEO12148.1), *Camptotheca acuminata* (AAB69727.1), *Capsicum annuum* (Q9XEL8.1), *Catharanthus roseus* (AAT52222.1), *Catharanthus roseus* (Q03163.1), *Clematis armandii* (AEU08408.1), *Coffea arabica* (ADR51242.1), *Cucumis melo* (BAA36291.1), *Dimocarpus longan* (AET72044.1), *Eucommia ulmoides* (AAV54051.1), *Euphorbia pekinensis* (ABK56831.1), *Gentiana lutea* (BAE92730.1), *Gentiana macrophylla* (AFN89599.1), *Gentiana macrophylla* (AFN89600.1), *Glycine max* (XP_003519474.1), *Gossypium hirsutum* (AAC05088.1), *Gossypium hirsutum* (AAC05089.1), *Hevea brasiliensis* (CAA38469.1), *Ligularia fischeri* (ABJ16394.1), *Litchi chinensis* (ABF56518.2), *Medicago truncatula* (XP_003629056.1), *Morus alba* (AAD03789.1), *Nicotiana attenuata* (AAO85554.1), *Nicotiana sylvestris* (Q01559.1), *Nicotiana tabacum* (AAB87727.1), *Nicotiana tabacum* (AAL54878.1), *Panax quinquefolium* (ACV65036.1), *Populus trichocarpa* (XP_002300544.1), *Populus trichocarpa* (XP_002301898.1), *Pyrus pyrifolia* (ACE80213.1), *Ricinus communis* (XP_002510732.1), *Salvia miltiorrhiza* (ACD37361.1), *Solanum chacoense* (AEX26934.1), *Solanum lycopersicum* (AAB62581.1), *Solanum lycopersicum* (P48022.1), *Solanum tuberosum* (AAA93498.1), *Solanum tuberosum* (BAB20771.1), *Antirrhinum majus* (ABV25900.1), *Vitis vinifera* (XP_002275827.1), *Withania somnifera* (HQ293119, *WsHMGR1*), *Withania somnifera* (GQ921845, *WsHMGR2*).

root of *W. somnifera* plant (Fig. 4D) in contrast to the reported *WsHMGR1* (HQ293119, 2010) that expressed more in flower and root. *WsHMGR1* and *WsHMGR2* were 71% similar at nucleotide level and 70% similar at amino acid level. *WsHMGR2* showed highest similarity to *C. annuum* HMGR2 (Q9XEL8.1) and hence was considered as different from *WsHMGR1* (HQ293119). *WsDXR2* (GQ921844) clustered with *WsDXR1* (JQ710679) (Fig. 3) and gene expression patterns were similar (Fig. 4E). These two isoforms were 95% similar at nucleotide level and 96% similar at amino acid level. Hence, to analyze the leaf carbon translocation, these two isoforms (*WsHMGR2* and *WsDXR2*) were taken forward. *WsDXR2* was similar to *N. tabacum* (DQ839130.1) and *N. benthamiana* (CAJ85787.1) DXRs.

Tissue and developmental stage specific expression

Three different withanolides (i.e. withaferin A, 12-deoxywithastramonolide and withanolide A) were analyzed in leaf and root tissues of young and mature plants of *W. somnifera* 'CIM Poshita', 6 and 12 weeks after germination (Fig. 4). A significant increase in all the metabolites was observed in both root and leaf with age. The metabolite, particularly that of withaferin A content in leaves was higher than withanolide A at both the stages

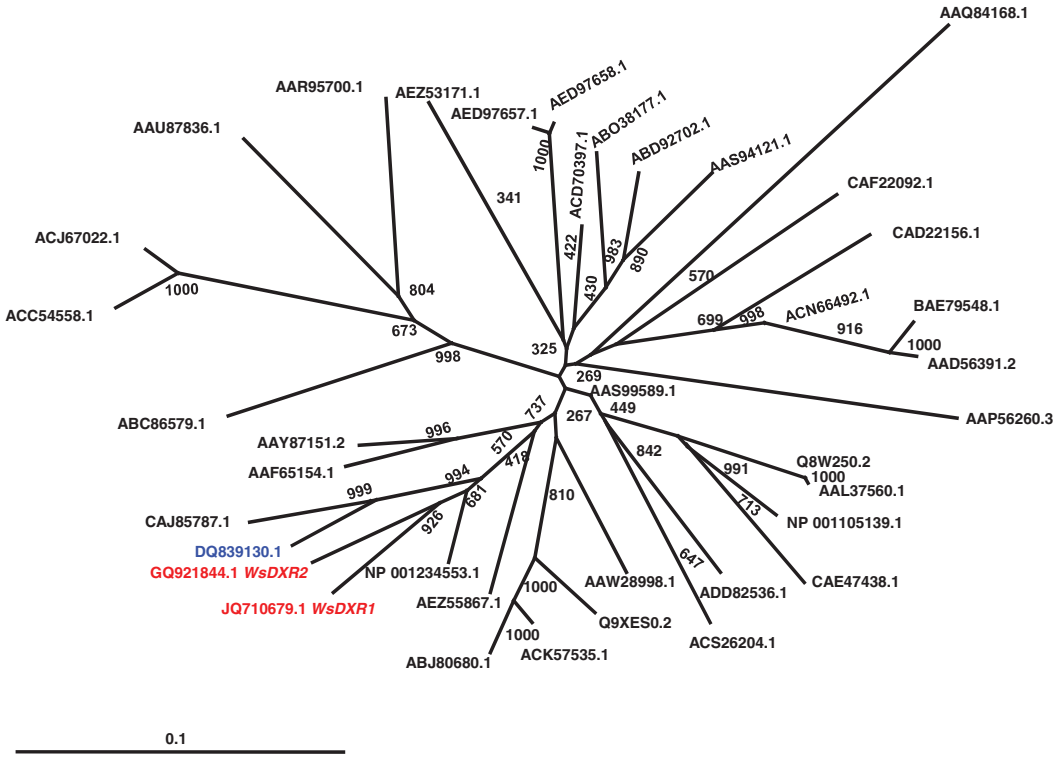

Fig. 3. Unrooted N-J tree comparing the amino acid sequences of *Withania somnifera* (*WsDXR2*) with *DXR*s reported from other species. GenBank accession numbers for the corresponding amino acid sequences are: *Ageratina adenophora* (ACN66492.1), *Amomum villosum* (ACS26204.1), *Antirrhinum majus* (AAW28998.1), *Arabidopsis thaliana* (AED97657.1), *Arabidopsis thaliana* (AED97658.1), *Artemisia annua* (AAD56391.2), *Camptotheca acuminate* (ABC86579.1), *Catharanthus roseus* (AAF65154.1), *Chrysanthemum morifolium* (BAE79548.1), *Cistus creticus* (AAP56260.3), *Croton stellatopilosus* (ABO38177.1), *Elaeis guineensis* (AAS99589.1), *Ginkgo biloba* (AAR95700.1), *Hevea brasiliensis* (AAS94121.1), *Hevea brasiliensis* (ABD92702.1), *Hordeum vulgare* (CAE47438.1), *Linum usitatissimum* (CAF22092.1), *Mentha piperata* (Q9XES0.2), *Mitragyna speciosa* (AEZ55867.1), *Narcissus tazetta* var. chinensis (ADD82536.1), *Nicotiana benthamiana* (CAJ85787.1), *Nicotiana tabacum* (DQ839130.1), *Oryza sativa* (AAL37560.1), *Oryza sativa japonica* (Q8W250.2), *Pinus densiflora* (ACC54558.1), *Pinus taeda* (ACJ67022.1), *Populus trichocarpa* (ACD70397.1), *Pueraria montana* (AAQ84168.1), *Rauvolfia verticillata* (AAY87151.2), *Rosa rugosa* (AEZ53171.1), *Salvia miltiorrhiza* (ABJ80680.1), *Salvia miltiorrhiza* (ACK57535.1), *Solanum lycopersicum* (NP_001234553.1), *Stevia rebaudiana* (CAD22156.1), *Taxus* × *media* (AAU87836.1), *Withania somnifera* (JQ710679, *WsDXR1*), *Withania somnifera* (GQ921844, *WsDXR2*), *Zea mays* (NP001105139.1).

of development (Fig. 4A, C). The *WsDXR2* transcript expression was more in leaf compared to root of young plant and the abundance in leaf also increased with age (Fig. 4D). Abundance of *WsHMGR2* transcripts in young root was slightly higher than the leaves of same stage but the expression increased in leaf at mature stage (Fig. 4D).

WsHMGR2 and *WsDXR2* transgenic tobacco lines

PCR analysis was carried out to verify the integration of transgene cassettes into the genome of transgenic lines. So the genomic DNA was PCR amplified from putative transgenic lines using primers designed from the CaMV35S promoter region (forward) and from the nos terminator region (reverse) flanking the gene (*WsDXR2* in case of pBI-*WsDXR2*, *WsHMGR2* in case of pBI-*WsHMGR2* and *GUS* for pBI121). The PCR results showed a 2486 bp amplicon in selected vector control transgenic line in which *GUS* (1811 bp) was present between the CaMV 35S promoter and *nos* terminator. A 2100 bp amplicon was observed for selected *WsDXR2* transgenic lines where *WsDXR2* gene (1425 bp) was ligated between the CaMV35S promoter and *nos* terminator. For *WsHMGR2* (1548 bp), the selected transgenic lines showed 2223 bp amplicon. No amplification was detected in untransformed wild type tobacco plants as expected (Fig. S1).

WsHMGR and *WsDXR* activity in transgenic tobacco lines

In addition to the transgenes from *W. somnifera*, the internal (endogenous tobacco) genes were also expected to show enzyme activity. However, expression of *WsDXR2* and *WsHMGR2* transgenes is controlled by CaMV 35S promoter whereas the tobacco gene(s) are subject to

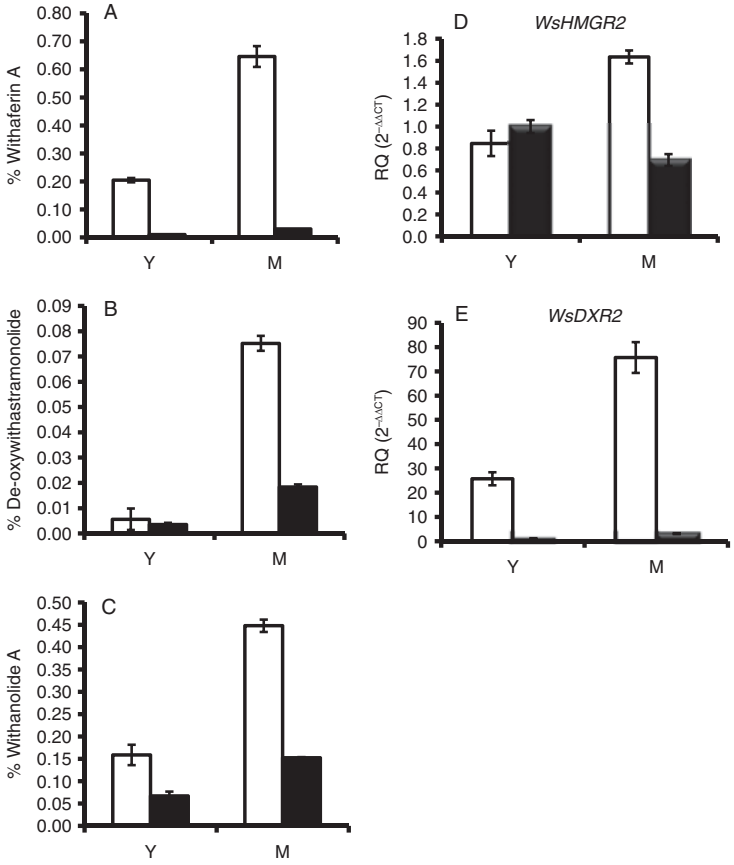

Fig. 4. Withanolides and transcript abundance analysis. Content (percent dry weight) of withaferin A (A), 12-deoxywithastramonolide (B), withanolide A (C) and expression pattern of *WsHMGR2* (D) and *WsDXR2* (E) transcripts in leaf (open boxes) and root tissue (closed dark boxes). Y, young plants 6 weeks after germination and M, mature plants 12 weeks after germination. RQ, relative quantity. Data are means ± SE (n = 3 biological replicates).

endogenous transcriptional and translational regulatory mechanisms. HMGR activity was monitored in the extract from the fresh leaves of plants that included the soluble and microsomal activities from the *WsHMGR2* transgenic lines displaying a high level of *WsHMGR2* mRNA (lines HMC1 and HMD1). The specific activity of HMGR in overexpressing plants was three- to sevenfolds higher compared to the vector control plants (Table 1A). Similarly, DXR activity was monitored in the stroma fraction of chloroplasts obtained from *WsDXR2* transgenic lines displaying a high level of *WsDXR2* mRNA (lines DXC1 and DXD1). The specific activity of DXR was 2.5–3-folds higher compared to the vector control plants (Table 1B).

Table 1. Enzyme activity in the transgenic tobacco plants: (A) HMGR activity and (B) DXR activity. [a]Specific activities are mean ± SD (n = 4 independent assays).

Plants	Specific activity[a] (nmol min^{-1} mg^{-1} protein)
A. *HMGR activity*	
HMC1	3.8 ± 0.566
HMD1	7.9 ± 1.273
Vector control	1.2 ± 0.212
B. *DXR activity*	
DXC1	16.6 ± 0.707
DXD1	12.9 ± 0.424
Vector control	5.58 ± 1.435

WsHMGR2 and *WsDXR2* expression in transgenic tobacco

The expression level of the transgenes was determined by semiquantitative PCR and quantitative RT-PCR. For this, three independent kanamycin-resistant *N. tabacum* transformants of pBI-*WsHMGR2* (HMB2, HMC1 and HMD1; Fig. 5A), three of pBI-*WsDXR2* (DXC1, DXD1 and DXD5; Fig. 5D) and one such transformant of pBI121 (Vector Control, VC) were chosen for semiquantitative PCR and quantitative RT-PCR analysis. Reactions were carried out with primers designed to specifically amplify the transgenes *WsHMGR2* and *WsDXR2* (Fig. 5B, E). All

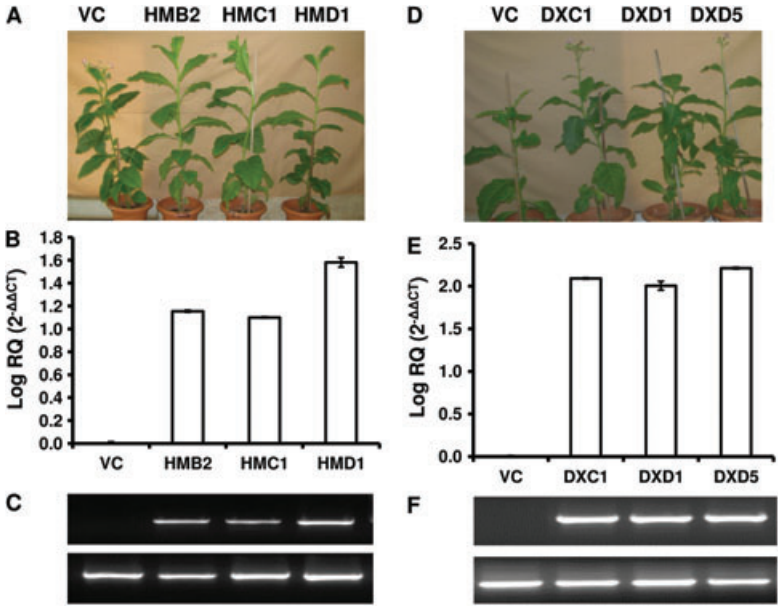

Fig. 5. Transgenic tobacco plants and analysis of *WsHMGR*2 and *WsDXR*2 expression. (A) Vector transformed plants (VC) compared to *WsHMGR*2 transformed tobacco lines HMB2, HMC1 and HMD1, (B) relative transcript quantity and (C) expression analysis through semiquantitative PCR. Similarly, (D), (E) and (F) shows vector transformed plants (VC) compared to *WsDXR*2 transformed tobacco lines DXC1, DXD1 and DXD5, relative transcript quantity and expression analysis through semiquantitative PCR respectively. Data are means ± SE (n = 3 biological replicates).

of the transformants of pBI-*WsHMGR2* and pBI-*WsDXR2* showed expression of *W. somnifera WsHMGR2* and *WsDXR2* respectively. The vector control (pBI121 with *GUS* gene only) did not show expression for either of the transgenes.

Sterol content in the leaves of transgenic tobacco lines

The effect of increased *WsHMGR2* and *WsDXR2* expression on sterol content was analyzed for sitosterol, stigmasterol, campesterol, cycloartenol and cholesterol from well expanded leaves of the transgenic tobacco plants. Higher quantity of cycloartenol, sitosterol, stigmasterol and campesterol was detected in plants overexpressing *WsHMGR2* compared to the transgenic plants overexpressing *WsDXR2* (Fig. 6). Though all the transgenic lines for both the genes expressed higher amount of these sterols, the increase was more significant in *WsHMGR2* transformed lines. About 200 and 88% increase in cycloartenol level was detected for *WsHMGR2* and *WsDXR2* transgenic tobacco lines respectively compared to the control. Similarly, the level of increase in sitosterol was about 160 and 25%, for stigmasterol 123 and 28%, and for campesterol it was 546 and 66% in *WsHMGR2* and *WsDXR2* transgenic tobacco lines respectively. In contrast, increase in the level of cholesterol was only marginally higher in *WsDXR2* (41%) compared to 38% in *WsHMGR2* lines.

Gene expression, sterol and withanolide content in transiently suppressed *W. somnifera* leaves

Transient RNAi experiments were undertaken with the prediction that knocking down *WsHMGR2* and *WsDXR2* will affect the concentration of corresponding withanolides and sterols depending upon the carbon contribution from MVA and MEP pathways. The real time expression analyses in plants infiltrated with pART27: *WsHMGR2i* and pART27: *WsDXR2i,* gene constructs showed reduced expression of *WsHMGR2* and *WsDXR2* compared to pART27 (only vector) infiltrated plants (Fig. 7A). A significant decrease in content of three withanolides was observed in the transiently silenced leaf tissue (Fig. 7B–D). A reduction of 87.2 and 56.8% in withaferin A content was observed in the *WsHMGR2* and *WsDXR2* suppressed tissues compared to the control plant infiltrated with pART27. The corresponding reduction in 12-deoxywithastramonolide was found to be 86.4% (*WsHMGR2*) and 54.5% (*WsDXR2* RNAi). Likewise, withanolide A reduced to the level of 58.7 and 56.2% in the *WsHMGR2* and *WsDXR2* suppressed tissue compared to control. Reduction of cycloartenol, campesterol, sitosterol and stigmasterol contents was also detected in the total leaf tissue infiltrated with

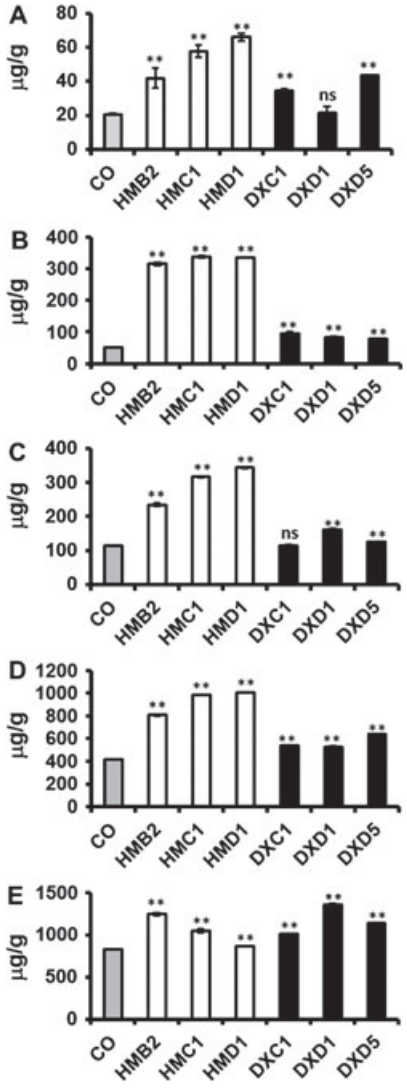

Fig. 6. Sterols in transgenic tobacco plants. Cycloartenol (A), campesterol (B), sitosterol (C), stigmasterol (D) and cholesterol (E) content in the leaf of *WsHMGR*2 (HMB2, HMC1 and HMD1) and *WsDXR*2 (DXC1, DXD1 and DXD5) transgenic tobacco lines compared to control untransformed tobacco plant (CO). Data are means ± SE (n = 3 biological replicates). $^{**}P < 0.01$ and $^{*}P < 0.05$; ns, not significant by Dunnett Multiple Comparisons Test.

pART27: *WsHMGR2i* compared to pART27: *WsDXR2i*, but reduction in cholesterol level was higher in the tissue infiltrated with pART27: *WsDXR2i* (Fig. 8).

Fosmidomycin and mevinolin inhibition

To validate the RNAi suppression data, mevinolin (inhibits specifically HMGR) and fosmidomycin (inhibits specifically DXR) were used to inhibit *WsHMGR2* and *WsDXR2*, with the rationale that withanolides and sterol flux will be decreased proportionately in the tissue depending on the contribution of intermediates from MVA and MEP pathway respectively. Decrease in withaferin A and withanolide A content was higher in case of mevinolin treated twigs compared to fosmidomycin treated plant (Fig. 9A, B) . About 12% decrease in withaferin A was detected when treated with fosmidomycin compared to 50% decrease for mevinolin. Similarly the decrease was 30 and 40% for withanolide A. For stigmasterol the corresponding decrease was 7 and 15% (Fig. 9D), whereas campesterol decreased by about 10 and 45% when treated with fosmidomycin and mevinolin respectively (Fig. 9E). Interestingly, cholesterol decreased by about 64 and 25% when treated with fosmidomycin and mevinolin, respectively (Fig. 9C).

Withanolides after sterol feeding

To ascertain the channeling of intermediates toward withanolide biosynthesis through specific sterol route, highly probable sterols identified from earlier experiments were used in feeding assays. This was carried out with the assumption that specific sterol involved en-route to withanolide biosynthesis will increase the withanolide level in the tissue, if fed exogenously. Significant increase in withaferin A and withanolide A content was observed when the leaf samples were fed with all the sterols except cholesterol (Fig. 10A, B). Highest amount of increase was detected for campesterol and stigmasterol.

Discussion

The introduction, stable transformation and expression of *W. somnifera WsHMGR2* and *WsDXR2* under the control of CaMV 35S promoter in transgenic tobacco resulted in altered sterol profiles. Increase in HMGR and DXR enzyme activity in transgenic tobacco lines having elevated *WsHMGR2* and *WsDXR2* levels of these transcripts, an increase in differential sterol accumulation was also observed. According to Schaller (2004) the plant cells have several sterol pathway end-products predominantly campesterol, sitosterol, stigmasterol and isofucosterol in genetically defined proportions. Generally, four major sterols could be found in tobacco and these are cholesterol, campesterol, stigmasterol and sitosterol (Stedman 1968). While analyzing the sterols Liu et al (2007) predicted a probable co-elution of cholesterol and tocopherol together in tobacco because of their close retention time. But in this study we could separate the two molecules (Figs S2 and S3). Over-expression of *HMGR* generally increased the amount of sterols in several transgenic plants (Chappell et al. 1995, Schaller et al. 1995, Harker et al. 2003, Enfissi et al. 2005, Hey et al. 2006). Our observation that the increase in the

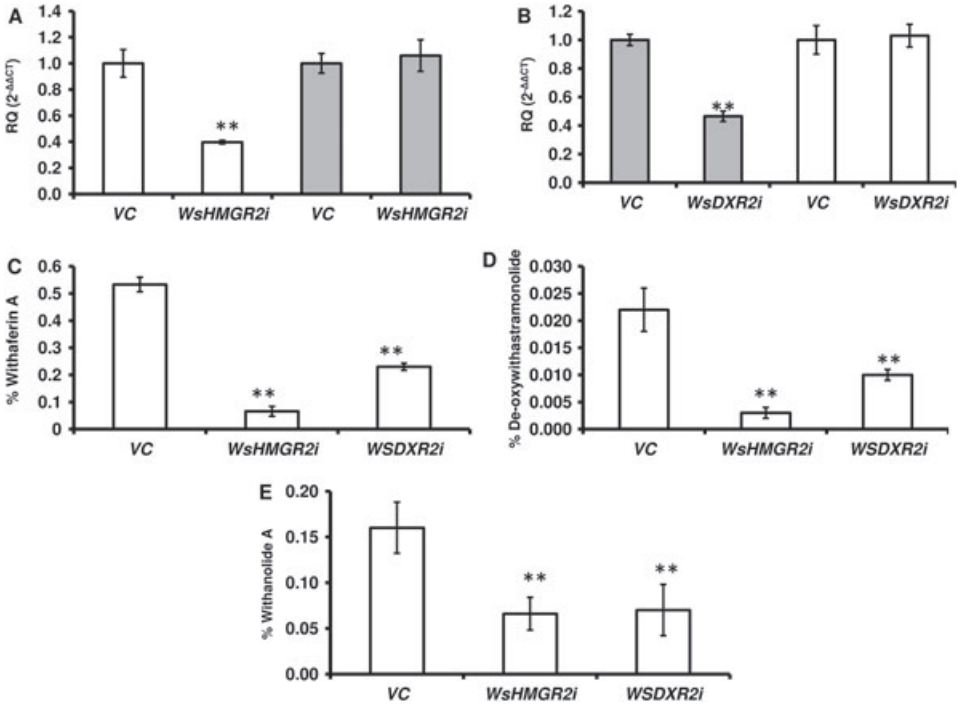

Fig. 7. Transcript abundance and withanolide content in transiently suppressed leaf samples of *Withania somnifera*. (A) Decrease in *WsHMGR2* expression (empty boxes) in pART27: *WsHMGR2i* (*WsHMGR2i*) infiltrated leaf samples compared to *WsDXR*2 expression (shaded boxes) and samples infiltrated with only vector pART27 (VC). (B) Decrease in *WsDXR2* expression (shaded boxes) in pART27: *WsDXR2i* (*WsDXR2i*) infiltrated leaf samples compared to *WsHMGR*2 expression (empty boxes) and samples infiltrated with only vector pART27 (VC). (C), (D) and (E) represent percent decrease in withaferin A, 12 Deoxywithastramonolide and withanolide A respectively in pART27: *WsHMGR2i* (*WsHMGR2i*) and pART27: *WsDXR2i* (*WsDXR2i*) infiltrated leaf samples compared to only vector pART27 (VC). Data are means ± SE (n = 3 biological replicates). $^{**}P < 0.01$ and $^{*}P < 0.05$; ns, not significant by Dunnett Multiple Comparisons Test.

accumulation of cycloartenol, campesterol, sitosterol and stigmasterol in leaf of *WsHMGR2* overexpressed plant was higher compared to the *WsDXR2* overexpressed plants where the increase in cholesterol was higher, excludes the possibility of lanosterol route for withanolide biosynthesis as proposed by Sangwan et al (2008) to be one of the options for withanolide biosynthesis. Less increase in cholesterol accumulation was observed in the leaf of *WsHMGR2* overexpressed plants. With an increase in 1.2 to 1.6 log RQ value of the transcript abundance there was an increase of three- to sevenfold in HMGR enzyme activity in the leaf of *WsHMGR2* overexpressed plants, whereas with a log RQ value of 2.0 to 2.2, the increase in DXR enzyme activity was about 2.5 to 3.0 folds compared to vector transformed plants. As it has been earlier suggested that the major changes in HMGR activity are determined at the transcriptional level and posttranslational changes contributes to the finer adjustments (Chappell et al. 1995), in our investigation, the transcript level of *WsDXR2* was found to be higher in transgenic plants compared to the vector control plants with a small increase in activity compared to the *WsHMGR2* transgenic plants. According to Rodríguez-Concepción et al. (2004), coordination of activities exists between MVA and MEP pathway to ensure the availability of isoprenoids for different end products through unknown mechanisms but a mutually exclusive pattern of expression between HMGR and DXR cannot be ruled out. Hasunuma et al. (2008) reported 2.5-fold higher sitosterol in the leaves of a transgenic tobacco line overexpressing *DXR* which according to them was the first example of increased sterol content intervaining the plastidial MEP pathway. However, the literature is scarce on sterol increase by *DXR* overexpression, in contrast to the *HMGR* which is generally accepted as the main rate-controlling step of the MVA pathway leading to sterol production. Hence, it may be possible that the overexpressed *WsDXR2* shows limited activity in the leaf as the native tobacco HMGR is already active and tuned to translocate carbon toward specific sterol biosynthesis. Also, the *WsHMGR2* transgene may complement the native gene of tobacco in contributing isoprene for the biosynthesis of mainly cycloartenol, campesterol, sitosterol and stigmasterol as observed in

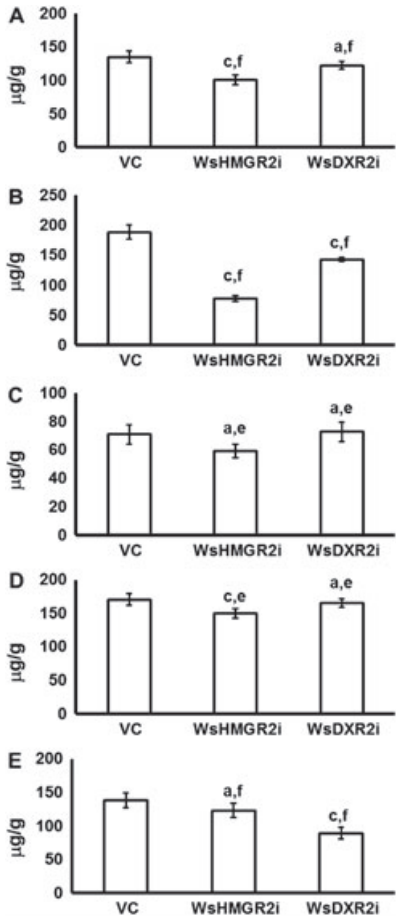

Fig. 8. Sterols in transiently suppressed leaf tissue of *Withania somnifera*. Cycloartenol (A), campesterol (B), sitosterol (C), stigmasterol (D) and cholesterol (E) content in transiently suppressed leaf of *W. somnifera* compared to samples infiltrated with only vector pART27 (VC). *WsHMGR2i* indicates sample infiltrated with pART27: *WsHMGR2i* and *WsDXR2i* indicates sample infiltrated with pART27: *WsDXR2i*. Data are means ± SE (n = 3 biological replicates). a, Non-significant, $P > 0.05$; b, significant, $P < 0.05$; c, significant, $P < 0.01$ compared to control and d, non-significant, $P > 0.05$; e, significant, $P < 0.05$; f, significant, $P < 0.01$ between *WsHMGR2i* vs *WsDXR2i* as analyzed by Tukey's test.

our study. Though the full modality of this preferential channeling cannot be explained at this point, but the accumulation of these sterols particularly campesterol and stigmasterol due to *WsHMGR2* overexpression indicates the possible channeling of carbon toward withanolide through these intermediates. Cycloartenol being the precursor for the end products campesterol and stigmasterol, and as sitosterol is converted to stigmasterol, cycloartenol and sitosterol may be excluded from carbon partitioning scheme in withanolides biosynthesis.

Since *HMGR* and *DXR* are essential housekeeping genes, it was difficult to retrieve RNAi transgenic plants. Hence a transient *Agrobacterium tumefaciens*-mediated plant expression system (Ratogi et al. 2013) was used by us to investigate the role of *WsDXR* and *WsHMGR* in the steroidal biosynthetic pathway of *W. somnifera* leading to withanolides production. The transient RNAi, though not comparable to stable transgenic results, still supported our finding in overexpression experiments. The fragment taken for *WsHMGR2* RNAi construct does not show much homology with *WsHMGR1*; Fig. S4). Hence the construct was assumed to be knocking down the expression of *WsHMGR2* only. *WsDXR1* and *WsDXR2* are highly homologous (96% at amino acid level) with similar expression patterns. The marginal difference in these two isoforms may be due to genotype effect as these isoforms were isolated from two independent genotypes (Fig. S5). Hence, these isoforms were assumed to be same genes performing similar function in the leaf. The results of this study indicated a relative decrease in withanolides content in transiently silenced tissues for both the genes, but the reduction in metabolite was more in pART27: *WsHMGR2i* construct infiltrated leaf compared to pART27: *WsDXR2i* infiltrated tissue with similar decrease in transcript abundance. Even if *WsDXR1* and *WsDXR2* are considered to be different isoform, inhibition of these might have presumably reduced the withanolide levels more than HMGR inhibition, if this gene is responsible in translocating the intermediates toward withanolide biosynthesis. But this was not the case, as the decrease in withanolides is more in *WsHMGR2* suppressed tissue compared to *WsDXR2* suppression. Cycloartenol, sitosterol, stigmasterol, campesterol, cholesterol decreased by 25, 16, 12, 59 and 11%, respectively in the pART27: *WsHMGR2i* infiltrated leaf and by 9, 0, 3, 24 and 35%, respectively in the pART27: *WsDXR2i* infiltrated tissue. The less reduction in the individual sterol levels may be due to dilution effect and non uniform infiltration as whole leaf tissue was analyzed instead of the selected infiltrated patches. But, nevertheless the decreasing trend indicated higher reduction of cholesterol when *WsDXR2* was suppressed and higher reduction of all other sterols when *WsHMGR2* was suppressed transiently. These results correlate with the overexpression results for individual sterols.

Plant HMGR is known to be controlled by a number of developmental and environmental signals like phytohormones, calcium, calmodulin, light, wounding, elicitor treatment and pathogen attack (Stermer et al. 1994). Hence, plants are not supposed to synthesize specific end product molecules in a fixed proportion from intermediates, channeled through MVA pathway. This is also true for intermediate translocation through MEP pathway. According to Hemmerlin et al (2012), under standard growth conditions, C20-phytyl moieties, C30-triterpenes and C40-carotenoids are made

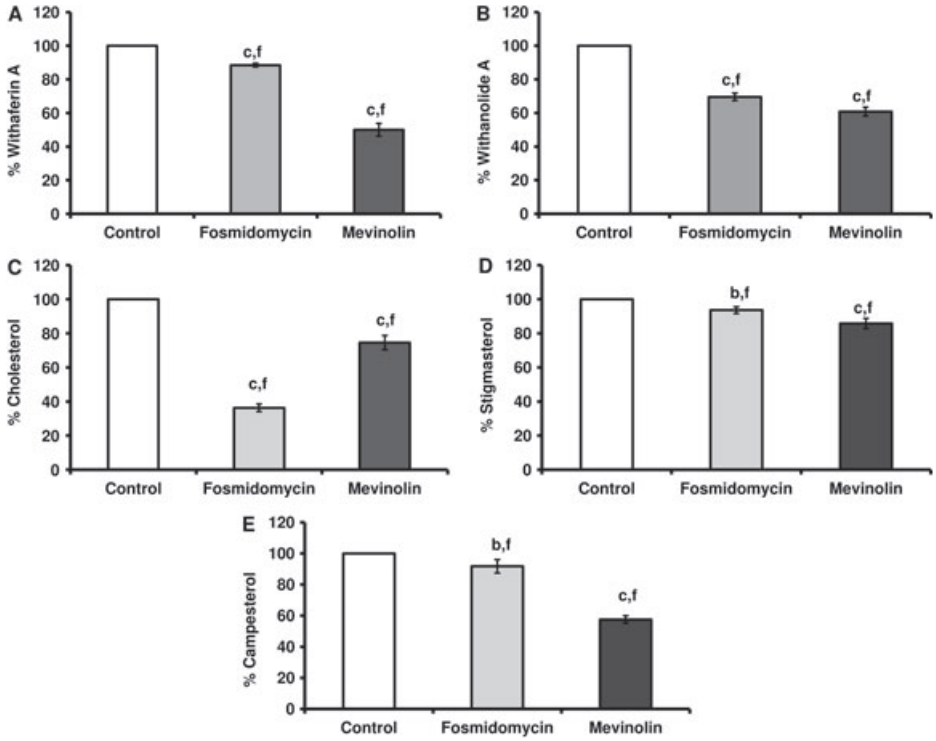

Fig. 9. Reduced biosynthesis of metabolites due to inhibition of MVA and MEP pathways by mevinolin and fosmidomycin respectively. Percent decrease of withaferin A (A), withanolide A (B), cholesterol (C), stigmasterol (D) and campesterol (E) compared to control (100%, Y-axis). Data are means ± SE (n = 3 biological replicates). a, Non-significant, $P > 0.05$; b, significant, $P < 0.05$; c, significant, $P < 0.01$ compared to control and d, non-significant, $P > 0.05$; e, significant, $P < 0.05$; f, significant, $P < 0.01$ between fosmidomycin vs mevinolin treatments as analyzed by Tukey's test.

nearly exclusively within compartmentalized pathways, while mixed origins are widespread for other types of isoprenoid-derived molecules in angiosperms. MEP pathway is reported to be partially contributing toward sitosterol in *Catharanthus roseus* cell culture (Arigoni et al. 1997), while equal contribution of MVA or MEP pathway was detected in *Croton sublyratus* callus culture (De-Eknamkul and Potduang 2003). So, when both pathways are operating in cross talk, it is difficult to maintain complete exclusivity of either pathway for a specific end product. However, despite the compartmentalization of these two pathways, MVA-derived precursors can be used for the synthesis of isoprenoids in the plastid, and MEP-derived precursors can be exported to the cytosol in at least some plants, tissues or/and developmental stages (Lichtenthaler 1999, Eisenreich et al. 2001, Rodríguez-Concepción et al. 2004). In this study also a substantial cross talking was observed during sterol biosynthesis with a clear differentiation of cholesterol on the one hand and cycloartenol on the other, where the latter is further converted to sitosterol, stigmasterol and campesterol. It has also been described that small amounts of sitosterol (1.5% relative to the cycloartenol pathway) was biosynthesized via lanosterol route (Ohyama et al. 2009), but considering the small contribution to sterol and large amount of withanolides in the leaf, it is logical to exclude the lanosterol route for withanolide biosynthesis.

HMGR inhibition with mevinolin reduced more amount of withanolides, stigmasterol and campesterol compared to DXR inhibition by fosmidomycin in *W. somnifera*. In contrast, fosmidomycin inhibition decreased the cholesterol biosynthesis more compared to mevinolin inhibition. When fed with different sterols, significant increase in withaferin A and withanolide A was detected for all sterols (cycloartenol, sitosterol, stigmasterol and campesterol) except cholesterol. So it is logical to expect the metabolite translocation predominately through campesterol and stigmasterol. Simultaneously, it is also predicted that the carbon contribution for these sterols vis a vis withanolides is of mixed origin with always greater contribution from MVP compared to MEP pathway. The proportion of contribution may be variable and decided by stage of tissue and environmental factors.

In summary, *WsHMGR2* predominantly diverts the flux toward cycloartenol with a lesser share toward lanosterol/cholesterol, whereas *WsDXR2* shifts the flux

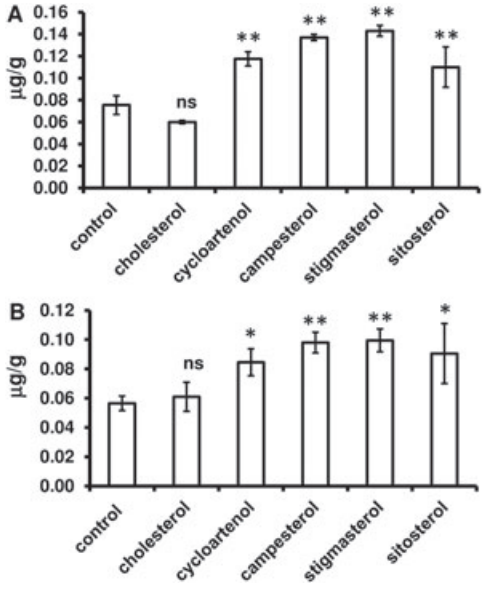

Fig. 10. Increase in withaferin A (A) and withanolide A (B) when fed with different sterols. Data are means ± SE (n = 3 biological replicates). $^{**}P < 0.01$ and $^{*}P < 0.05$; ns, not significant by Dunnett Multiple Comparisons Test.

toward lanosterol/cholesterol with less contribution for cycloartenol and other sterols biosynthesized from it. This was proved in overexpression, RNAi, using specific inhibitors for HMGR and DXR, and sterol feeding experiments in our study. Though, major source of withanolides in *W. somnifera* has been reported to be the leaf (Glotter 1991, Jayaprakasam and Nair 2003, Mirjalili et al. 2009) and the role of plastidial MEP pathway in their biosynthesis is evident, still the MVA pathway is the predominant pathway contributing these withanolides either through campesterol or stigmasterol. Also, considering the high accumulation of campesterol and stigmasterol in *WsHMGR2* overexpressed tobacco, comparatively higher reduction of these sterols along with withanolides in transiently suppressed *W. somnifera*, inhibiting HMGR and DXR, and higher increase of withanolides by feeding these sterols, the predominant route for withanolide biosynthesis can be indicated to be through campesterol/stigmasterol route. The mechanism behind variable contribution of these two pathways for different sterols and withanolides constitutes an interesting subject for future research in *W. somnifera*.

Accession numbers

Sequence data present in this study can be found in GenBank database (www.ncbi.nlm.nih.gov) of NCBI under the accession numbers *WsHMGR2* (GQ921845) and *WsDXR2* (GQ921844).

Author contributions

S. S. and S. P. have helped in experimentation and analysis; K. S. and C. S. C. have helped in sterol experiment and analysis; M. M. G. has helped in withanolide experiment and analysis; U. N. D. has helped in analysis and manuscript writing; A. K. S. has helped in planning, experimentation; analysis, interpretation and manuscript writing.

Acknowledgements – The authors express their sincere gratitude to the Director, CIMAP for his keen interest and providing facilities for the experiments. The seed and plant material was provided by NGBMAP. The help from Dr A K Mathur, Chief Scientist, CSIR-CIMAP in editing the manuscript is gratefully acknowledged. Help from Dr (Ms) N. S. Sangwan for fosmidomycin and mevinolin; Dr Atul Gupta for Estrone crucial for the experiments was acknowledged. This work was supported by CSIR-Central Institute of Medicinal and Aromatic Plants, Lucknow-226015 from the TFYP plan projects of CSIR (BSC0203). S. S. and S. P. (AcSIR) were supported by CSIR-SRF.

References

Akhtar N, Gupta P, Sangwan NS, Sangwan RS, Trivedi PK (2012) Cloning and functional characterization of 3-hydroxy-3-methylglutaryl coenzyme A reductase gene from *Withania somnifera*: an important medicinal plant. Protoplasma 250: 613–622

Arigoni D, Sagner S, Latzel C, Eisenreich W, Bacher A, Zenk MH (1997) Terpenoid biosynthesis from 1-deoxy-D-xylulose in higher plants by intramolecular skeletal rearrangement. Proc Natl Acad Sci USA 94: 10600–10605

Botella-Pavia P, Besumbes O, Phillips MA, Carretero-Paulet L, Boronat A, Rodríguez-Concepción M (2004) Regulation of carotenoid biosynthesis in plants: evidence for a key role of hydroxymethylbutenyl diphosphate reductase in controlling the supply of plastidial isoprenoid precursors. Plant J 40: 188–199

Bradford MM (1976) A rapid and sensitive method for the quantitation of microgram quantities of protein utilizing the principle of protein–dye binding. Anal Biochem 72: 248–254

Carretero-Paulet L, Cairo A, Botella-Pavıa P, Besumbes O, Campos N, Boronat A, Rodrıguez-Concepcion M (2006) Enhanced flux through the methylerythritol 4-phosphate pathway, in *Arabidopsis* plants overexpressing deoxyxylulose 5-phosphate,reductoisomerase. Plant Mol Biol 62: 683–695

Chappell J, Wolf F, Proulx J, Cuellar R, Saunders C (1995) Is the reaction catalyzed by 3-hydroyl-3-methlyglutaryl coenzyme A reductase a rate-limiting step for isoprenoid biosynthesis in plants? Plant Physiol 109: 1337–1343

Chaurasiya ND, Sangwan NS, Sabir F, Misra LN, Sangwan RS (2012) Withanolide biosynthesis recruits both mevalonate and DOXP pathways of isoprenogenesis in Ashwagandha *Withania somnifera* L. (Dunal). Plant Cell Rep 31: 1889–1897

Darnet S, Rahier A (2004) Plant sterol biosynthesis: identification of two distinct families of sterol 4 alpha-methyl oxidases. Biochem J 378: 889–898

De-Eknamkul W, Potduang B (2003) Biosynthesis of beta-sitosterol and stigmasterol in *Croton sublyratus* proceeds via a mixed origin of isoprene units. Phytochemistry 62: 389–398

Dhuley JN (2001) Nootropic-like effect of Ashwagandha (*Withania somnifera L.*) in mice. Phytother Res 15: 524–528

Dubey VS, Bhalla R, Luthra R (2003) An overview of the nonmevalonate pathway for terpenoid biosynthesis in plants. J Biosci 28: 637–646

Eisenreich W, Rohdich F, Bacher A (2001) Deoxyxylulose phosphate pathway to terpenoids. Trends Plant Sci 6: 78–84

Enfissi EMA, Fraser PD, Lois LM, Boronat A, Schuch W, Brambley PM (2005) Metabolic engineering of the mevalonate and non-mevalonate isopentenyl diphosphate-forming pathways for the production of health-promoting isoprenoids in tomato. Plant Biotechnol J 3: 17–27

Ge X, Wu J (2005) Tanshinone production and isoprenoid pathways in *Salvia miltiorrhiza* hairy roots induced by Ag^+ and yeast elicitor. Plant Sci 168: 487–491

Glotter E (1991) Withanolides and related ergostane-type steroids. Nat Prod Rep 8: 415–440

Gupta GL, Rana AC (2007) *Withania somnifera* (ashwagandha): a review. Pharmacol Rev 1: 129–136

Gupta P, Akhtar N, Tewari SK, SangwanRS TPK (2011) Differential expression of farnesyl diphosphate synthase gene from *Withania somnifera* in different chemotypes and in response to elicitors. Plant Growth Regul 65: 93–100

Gupta P, Agarwal AV, Akhtar N, Sangwan RS, Singh SP, Trivedi PK (2013a) Cloning and characterization of 2-C-methyl-D-erythritol-4-phosphate pathway genes for isoprenoid biosynthesis from Indian ginseng, *Withania somnifera*. Protoplasma 250: 285–295

Gupta P, Goel R, Pathak S, Srivastava A, Singh SP, Sangwan RS, Asif MH, Trivedi PK (2013b) *De novo* assembly, functional annotation and comparative analysis of *Withania somnifera* leaf and root transcriptomes to identify putative genes involved in the withanolides biosynthesis. PLoS One 8: e62714

Harker M, Holmberg N, Calyton JC, Gibbard CL, Wallace AD, Rawlins S, Hellyer SA, Lanot A, Safford R (2003) Enhancement of seed phytosterol levels by expression of an N-terminal truncated *Hevea brasiliensis* (rubber tree) 3-hydroxy-3-methylglutaryl-CoA reductase. Plant Biotechnol J 1: 113–121

Hasunuma T, Takeno S, Hayashi S, Sendai M, Bamba T, Yoshimura S, Tomizawa K, Fukusaki E, Miyake C (2008) Overexpression of 1-deoxy-D-xylulose-5-phosphate reductoisomerase gene in chloroplast contributes to increment of isoprenoid production. J Biosci Bioeng 105: 518–526

Hemmerlin A, Harwood JL, Bach TJ (2012) A raison d'être for two distinct pathways in the early steps of plant isoprenoid biosynthesis? Prog Lipid Res 51: 95–148

Hey SJ, Powers SJ, Beale MH, Hawkins ND, Ward JL, Halford NG (2006) Enhanced seed phytosterol accumulation through expression of a modified HMG-CoA reductase. Plant Biotechnol J 4: 219–229

Horsch RB, Fry JE, Hoffmann NL, Eichholtz D, Rogers SG, Fraley RT (1985) A simple and general method for transferring genes into plants. Science 227: 1229–1231

Jayaprakasam B, Nair MG (2003) Cyclooxygenase-2 enzyme inhibitory withanolides from *Withania somnifera* leaves. Tetrahedron 59: 841–849

Kahn RA, Bak S, Olsen CE, Svendsen I, Moller BL (1996) Isolation and reconstitution of the heme-thiolate protein obtusifoliol 14 alpha-demethylase from *Sorghum bicolor* (L.) Moench. J Biol Chem 271: 32944–32950

Lichtenthaler HK (1999) The 1-deoxy-D-xylulose-5-phosphate pathway of isoprenoid biosynthesis in plants. Annu Rev Plant Physiol Plant Mol Biol 50: 47–65

Liu WH, Ding B, Ruan XM, Xu HT, Yang J, Liu SM (2007) Analysis of free and conjugated phytosterols in tobacco by an improved method using gas chromatography–flame ionization detection. J Chromatogr A 1163: 304–311

Lockley WJS, Rees HH, Goodwin TW (1976) Biosynthesis of steroidal withanolides in *Withania somnifera*. Phytochemistry 15: 937–939

Luo K, Zheng X, Chen Y, Xiao Y, Zhao D, McAvoy R, Pei Y, Li Y (2006) The maize *Knotted1* gene is an effective positive selectable marker gene for *Agrobacterium*-mediated tobacco transformation. Plant Cell Rep 25: 403–409

Madina BR, Sharma LK, Chaturvedi P, Sangwan RS, Tuli R (2007) Purification and characterization of a novel glucosyltransferase specific to 27 β-hydroxy steroidal lactones from *Withania somnifera* and its role in stress responses. Biochim Biophys Acta 1774: 1199–1207

Mansouri H, Asrar Z, Mehrabani M (2009) Effects of gibberellic acid on primary terpenoids and Δ^9-tetrahydrocannabinol in *Cannabis sativa* at flowering stage. J Int Plant Biol 51: 553–561

Miller B, Heuser T, Zimmer W (2000) Functional involvement of a deoxy-D-xylulose 5-phosphate reductoisomerase gene harboring locus of *Synechococcus leopoliensis* in isoprenoid biosynthesis. FEBS Lett 481: 221–226

Mirjalili MH, Moyano E, Bonfil M, Cusido RM, Palazon J (2009) Steroidal lactones from *Withania somnifera*, an ancient plant for novel medicine. Molecules 14: 2373–2393

Misra L, Mishra P, Pandey A, Sangwan RS, Sangwan NS, Tuli R (2008) Withanolides from *Withania somnifera* roots. Phytochemistry 69: 1000–1004

Misra A, Chanotiya CS, Gupta MM, Dwivedi UN, Shasany AK (2012) Characterization of cytochrome P450 monooxygenases isolated from trichome enriched fraction of *Artemisia annua* L. leaf. Gene 510: 193–201

Ohyama K, Suzuki M, Kikuchi J, Saito K, Muranaka T (2009) Dual biosynthetic pathways to phytosterol *via* cycloartenol and lanosterol in *Arabidopsis*. Proc Natl Acad Sci USA 106: 725–730

Pal S, Singh S, Shukla AK, Gupta MM, Khanuja SPS, Shasany AK (2011) Comparative withanolide profiles, gene isolation, and differential gene expression in the leaves and roots of *Withania somnifera*. J Hortic Sci Biotechnol 86: 391–397

Pandey V, Misra P, Chaturvedi P, Mishra MK, Trivedi PK, Tuli R (2010) *Agrobacterium tumefaciens*-mediated transformation of *Withania somnifera* (L.) Dunal: an important medicinal plant. Plant Cell Rep 29: 133–141

Ratogi S, Kumar R, Chanotiya CS, Shanker K, Gupta MM, Nagegowda DA, Shasany AK (2013) 4-Coumarate:CoA ligase partitions metabolites for eugenol biosynthesis. Plant Cell Physiol 54: 1238–1252

Ray AB, Gupta M (1994) Withasteroids – a growing group of naturally occurring steroidal lactones. Prog Chem Org Nat Prod 63: 1–106

Rodríguez-Concepción M, Forés O, Martínez-García JF, González V, Phillips MA, Ferrer A, Boronat A (2004) Distinct light-mediated pathways regulate the biosynthesis and exchange of isoprenoid precursors during *Arabidopsis* seedling development. Plant Cell 16: 144–156

Rohmer M (1999) The discovery of a mevalonate-independent pathway for isoprenoid biosynthesis in bacteria, algae and higher plants. Nat Prod Rep 16: 565–574

Saitou N, Nei M (1987) The neighbor-joining method: a new method for reconstructing phylogenetic trees. Mol Biol Evol 4: 406–425

Sangwan RS, Chaurasiya ND, Lal P, Misra L, Tuli R, Sangwan NS (2008) Root-contained withanolide A is inherently *de novo* synthesized within roots in Ashwagandha (*Withania somnifera*). Physiol Plant 133: 278–287

Scartezzini (2007) Genetic and phytochemical difference between some Indian and Italian plants of *Withania somnifera* (L.) Dunal. Nat Prod Res 21: 923–932

Schaller H (2004) New aspects of sterol biosynthesis in growth and development of higher plants. Plant Physiol Biochem 42: 465–476

Schaller H, Grausem B, Benveniste P, Chye ML, Tan CT, Song YH, Chua NH (1995) Expression of the *Hevea brasiliensis* (H.B.K.) Müll. Arg 3-hydroxy-3-methlyglutaryl-coenzyme A reductase 1 in tobacco results in sterol overproduction. Plant Physiol 109: 761–770

Senthil K, Wasnik NG, Kim YJ, Yang DC (2010) Generation and analysis of expressed sequence tags from leaf and root of *Withania somnifera* (Ashwagandha). Mol Biol Rep 37: 893–902

Sharma LK, Madina BR, Chaturvedi P, Sangwan RS, Tuli R (2007) Molecular cloning and characterization of one member of 3 beta-hydroxy sterol glucosyltransferase gene family in *Withania somnifera*. Arch Biochem Biophys 460: 48–55

Srivastava P, Tiwari N, Yadav AK, Kumar V, Shanker K, Verma RK, Gupta MM, Gupta AK, Khanuja SPS (2008) Simultaneous quantification of withanolides in *Withania somnifera* by a validated high-performance thin-layer chromatographic method. J AOAC Int 91: 1154–1161

Stedman RL (1968) The chemical composition of tobacco and tobacco smoke. Chem Rev 68: 153–207

Stermer BA, Bianchini GM, Korth KL (1994) Regulation of HMG-CoA reductase activity in plants. J Lipid Res 35: 1133–1140

Suzuki M, Muranaka T (2007) Molecular genetics of plant sterol backbone synthesis. Lipids 42: 47–54

Takahashi S, Kuzuyama T, Watanabe H, Seto H (1998) A 1-deoxy-D-xylulose 5-phosphate reductoisomerase catalyzing the formation of 2-C-methyl-D-erythritol 4-phosphate in an alternative nonmevalonate pathway for terpenoid biosynthesis. Proc Natl Acad Sci USA 95: 9879–9884

Thompson JD, Gibson TJ, Plewniak F, Jeanmougin F, Higgins DG (1997) The CLUSTAL_X Windows interface: flexible strategies for multiple sequence alignment aided by quality analysis tools. Nucl Acids Res 25: 4876–4882

Toroser D, Huber S (1998) 3-Hydroxy-3-methylglutaryl-coenzyme A reductase kinase and sucrose–phosphate synthase kinase activities in cauliflower florets: Ca^{2+}dependence and substrate specificities. Arch Biochem Biophys 355: 291–300

Velde VV, Lavie D (1982) A Δ^{16}-withanolide in *Withania somnifera* as a possible precursor for α-side-chains. Phytochemistry 21: 731–733

Winters M (2006) Ancient medicine and modern use: *Withania somnifera* and its potential role in integrative oncology: a review. Altern Med Rev 11: 269–277

Supporting Information

Additional Supporting Information may be found in the online version of this article:

Appendix S1. List of primers used in this investigation.

Figure S1. PCR analysis indicating the transfer of transgene cassette into the tobacco plants. Lane M: λ DNA *Eco*RI/ *Hin*dIII digest, Lane W: Amplification of untransformed plant DNA, Lane V: Amplification of vector transformed plant DNA, Lanes HMB2, HMC1 and HMD1 denotes amplified DNA from *WsHMGR*2 transformed plant lines, Lanes DXC1, DXD1 and DXD5 have amplified DNA from *WsDXR*2 transformed plant lines. The cassette was amplified with primers from CaMV35S promoter and *nos* terminator. Hence, untransformed plant DNA does not show amplification, vector transformed plant DNA shows 2486 bp amplicon where as *WsHMGR*2 transformed plant lines show 2223 bp amplicons and *WsDXR*2 shows 2100 bp amplicons.

Figure S2. GC chromatograms of (A) cholesterol (Ch); (B) tocopherol (To) and (C) cholesterol and tocopherol mixture injected together.

Figure S3. Representative GC chromatograms showing (A) standards for estrone (ES), cholesterol (Ch), campesterol (Ca), stigmasterol (St), sitosterol (Si), cycloartenol (cy); (B) sterols from vector transformed plant; (C) plant transformed with *WsHMGR2*; (D) plant transformed with *WsDXR2*. The right-hand panel shows GC-MS profiles of different sterols analyzed in this investigation.

Figure S4. Multiple sequence alignment of *HMGR*s showing RNAi fragment and the primer position for semiquantitative PCR analysis.

Figure S5. Multiple sequence alignment of *DXR*s showing RNAi fragment and the primer position for semiquantitative PCR analysis.

Edited by E. Pesquet